Schottky contacts to In_2O_3

Cite as: APL Mater. **2**, 046104 (2014); https://doi.org/10.1063/1.4870536
Submitted: 08 January 2014 . Accepted: 26 March 2014 . Published Online: 04 April 2014

H. von Wenckstern, D. Splith, F. Schmidt, M. Grundmann, O. Bierwagen, and J. S. Speck

Schottky contacts to In_2O_3

H. von Wenckstern,[1,a] D. Splith,[1] F. Schmidt,[1] M. Grundmann,[1]
O. Bierwagen,[2,3] and J. S. Speck[3]
[1]*Universität Leipzig, Fakultät für Physik und Geowissenschaften, Institut für Experimentelle Physik II, Linnéstrasse 5, 04103 Leipzig, Germany*
[2]*Paul Drude Institut für Festkörperelektronik, Hausvogteiplatz 5-7, 10117 Berlin, Germany*
[3]*Materials Department, University of California, Santa Barbara, California 93106, USA*

(Received 8 January 2014; accepted 26 March 2014; published online 4 April 2014)

n-type binary compound semiconductors such as InN, InAs, or In_2O_3 are especial because the branch-point energy or charge neutrality level lies within the conduction band. Their tendency to form a surface electron accumulation layer prevents the formation of rectifying Schottky contacts. Utilizing a reactive sputtering process in an oxygen-containing atmosphere, we demonstrate Schottky barrier diodes on indium oxide thin films with rectifying properties being sufficient for space charge layer spectroscopy. Conventional non-reactive sputtering resulted in ohmic contacts. We compare the rectification of Pt, Pd, and Au Schottky contacts on In_2O_3 and discuss temperature-dependent current-voltage characteristics of Pt/In_2O_3 in detail. The results substantiate the picture of oxygen vacancies being the source of electrons accumulating at the surface, however, the position of the charge neutrality level and/or the prediction of Schottky barrier heights from it are questioned. [http://dx.doi.org/10.1063/1.4870536]

Semiconducting oxides (SO) find application in transparent electrodes for thin film solar cells, as rectifiers, as transistors, as UV-photodetectors, and as chemical, gas and pH-sensors. In order to realize devices with optimized performance, the bulk as well as the surface properties of the SO-layers must be controllable and adjustable. In_2O_3 thin films with high room temperature (RT) mobilities (up to 230 $cm^2/V\,s$[1,2]) and controllable conductivities ranging from semi-insulating (by Mg-doping[3]) to highly conductive (by Sn-doping[4]) have favorable bulk transport properties for transistor applications. However, especially the surface electron accumulation layer (SEAL) of SOs is difficult to modify and in some cases like for In_2O_3 not sufficiently tunable to allow the formation of Schottky contacts. King *et al.* explained the surface electron accumulation as well as the ease of extrinsic *n*-type doping of In_2O_3 by the position of the branch point energy E_{bp} (sometimes referred to as charge neutrality level) within the conduction band and about 0.4 eV above the conduction band minimum (CBM).[5] Recently, a value of 0.35 eV above CBM was derived by quasi-particle calculations in close agreement with the experimental value.[6] The microscopic origin of surface electrons is likely the formation of oxygen vacancies at the topmost surface layer(s).[7,8] A remote oxygen plasma treatment was capable of removing the electron accumulation at the surface of ZnO[9,10] and allowed the fabrication of Schottky contacts with acceptable rectification thereon. Qualitatively the same results have been obtained with SnO_2 films by an oxygen plasma treatment of the surface.[11,12] For In_2O_3, Bierwagen and co-workers investigated the change of the surface band bending due to the same oxygen plasma treatment by x-ray photoemission spectroscopy.[13] As-grown samples showed a downward band bending (surface Fermi level is above conduction band minimum) independent of the growth conditions. The oxygen plasma treatment reversed the band bending at the surface such that an upward bending was observed after the treatment, however,

[a]wenckst@physik.uni-leipzig.de. URL: www.uni-leipzig.de/~wenckst.

current-voltage (*IV*) characteristics of mercury (Hg) contacts remained poor. Here we present a proof of principle study demonstrating that a reactive sputtering process of the Schottky contact metal in an oxygen-containing ambient addresses the obstacles for fabrication of Schottky barrier diodes on In_2O_3 and show its suitability for the fabrication of Schottky diodes on In_2O_3(001) thin films grown by molecular beam epitaxy (MBE). The rectification achieved is sufficient for space charge spectroscopic characterization methods.

Three approximately 500 nm-thick In_2O_3(001) films were grown by plasma-assisted molecular beam epitaxy on (001)-oriented yttria-stabilized zirconia (YSZ) substrates. These films comprise an unintentionally doped (UID) film, a lightly Mg-doped film with Mg concentration of $N_{Mg} = 1.3 \times 10^{17}\,cm^{-3}$, and a lightly Sn-doped film with Sn concentration of $N_{Sn} = 10^{18}\,cm^{-3}$. Details on Mg and Sn-doping are described in Refs. 3 and 4, respectively. Differences in the post-growth cool-down conditions in the MBE chamber (oxygen plasma or vacuum), and their respective consequences on oxygen-related defects,[1,3,4] were equalized by annealing the samples for 1 min at 750 °C in air prior to contact deposition. Standard photolithography was used to pattern ohmic and circular Schottky contacts. For ohmic contacts gold was dc-sputtered under Ar atmosphere. RT Hall effect measurements were performed at a magnetic field of 0.43 T. Here, ohmic contacts were placed at the corners of square-shaped $5 \times 5\,mm^2$ samples. For the creation of Schottky contacts sputtering in Ar was not successful independent of the contact metal used. Similar to former reports for ZnO we applied reactive dc-sputtering of Au, Pd, and Pt.[14–16] The gas flow of 50 vol.% argon and 50 vol.% oxygen was 100 standard cubic centimeter per minute resulting in a total pressure of 0.025 mbar during the sputtering process. The target diameter is 30 mm, the target-to-substrate distance was 4 cm and a sputtering power of 30 W was used. The properties of the different contact metals are compared by means of RT *IV* measurements conducted in a SUESS probe station P200 connected to an Agilent Semiconductor Parameter Analyzer 4155C. For each metal an ensemble of 30 contacts or more was investigated per sample. For selected diodes the *IV* measurements were recorded in a temperature range from 293 K to 443 K.

Hall effect measurements on the annealed samples yielded free electron concentration n and the Hall mobility μ_H. The RT values are $n = 1.9 \times 10^{17}\,cm^{-3}$ and $\mu_H = 201\,cm^2/V\,s$ for the UID, $n = 1.6 \times 10^{17}\,cm^{-3}$ and $\mu_H = 147\,cm^2/V\,s$ for the Mg-doped and $n = 8.5 \times 10^{17}\,cm^{-3}$ and $\mu_H = 140\,cm^2/V\,s$ for the Sn-doped sample. As expected, the free electron concentration is highest for the Sn-doped and lowest for the Mg-doped sample; Hall mobility is highest for the UID sample and lowest for the Sn-doped sample.

Similar to evaporated metal contacts to SnO_2 described already in the literature[11] we could not observe a rectifying behavior for non-reactively dc-sputtered Au, Pd, and Pt on In_2O_3. In Fig. 1(a) the characteristic of a non-reactively sputtered Pt contact on the UID sample is shown exemplarily (see grey line in the figure) for all metal contacts that were realized that way on each sample type. None of these contacts showed rectification. Rectifying contacts were obtained by reactive sputtering of the respective metal as depicted in Fig. 1(a) for the case of Pt. A detailed microscopic understanding of Schottky contact formation does not exist so far. We speculate that, similar to the oxygen plasma treatment reported by Bierwagen and co-workers,[13] negative oxygen ions impinge the sample surface at the very beginning of the sputtering process. These oxygen ions might fill surface and surface-near oxygen vacancies, by that remove the origin of the SEAL, and move the surface Fermi level below the CBM. Positively charged argon ions simultaneously ablate the metal target such that the cleaned In_2O_3 surface is covered right away by the Schottky contact metal. Best room temperature current-voltage characteristics of reactively sputtered Au, Pd, and Pt contacts are depicted in Fig. 1 for the UID, the Mg-, and the Sn-doped sample with corresponding fits. For the fit we assumed that current transport across the barrier is due to thermionic emission, only (see the supplementary material for more details[19]).

Temperature-dependent current-voltage characteristics were measured for upward and downward temperature ramping for Pt/In_2O_3 in air between RT and 150 °C and are shown and discussed in the supplementary material.[19] At a temperature of 120 °C (393 K) a strong increase of the diode current is observed. At this temperature the barrier properties change. The series resistance of the diode decreased such that the current under flat-band conditions is now similar to that of Au Schottky barrier diodes. Further, the RT barrier height and the ideality factor are lower after the temperature

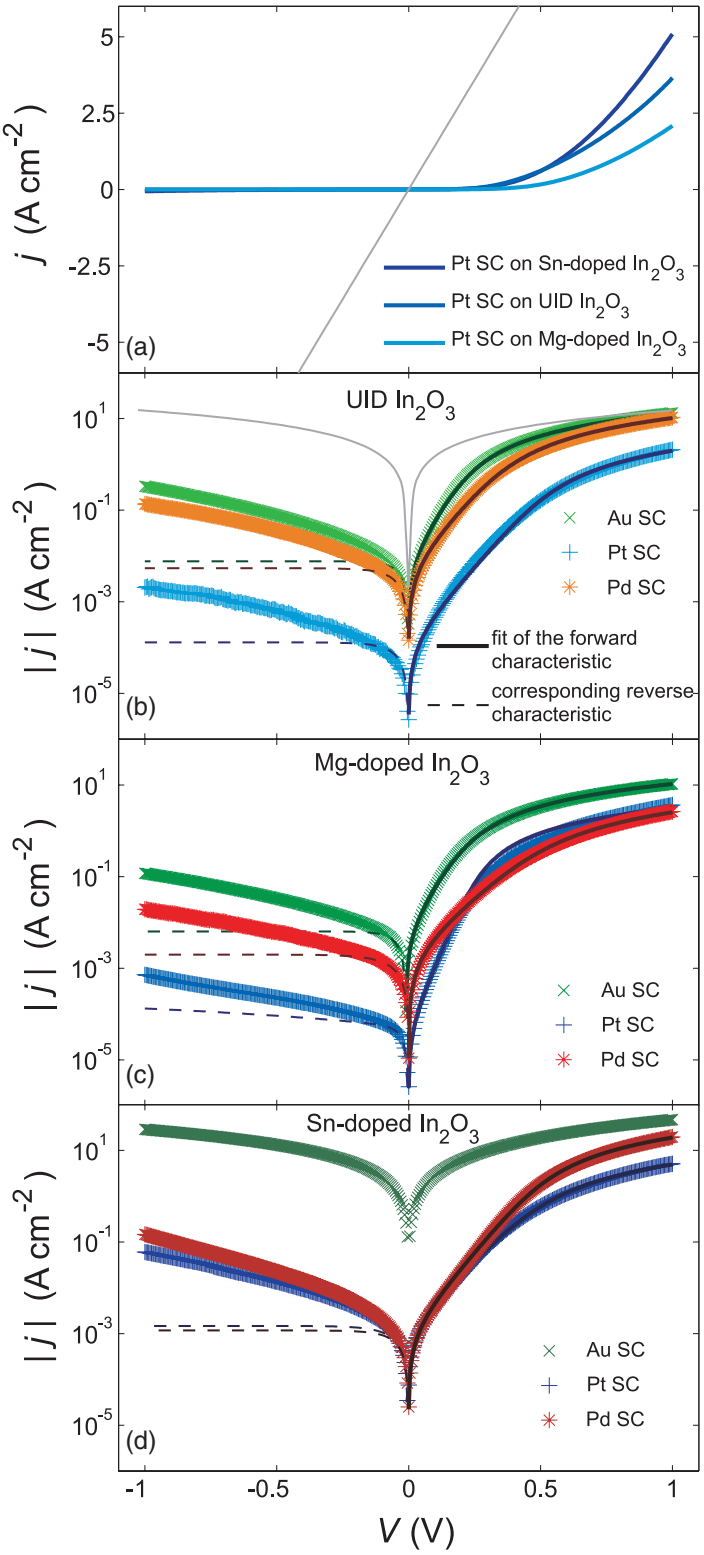

FIG. 1. (a) Comparison of room temperature $j(V)$-characteristics of reactively sputtered Pt Schottky barrier contacts on UID, Mg-, and Sn-doped In_2O_3 thin films. The grey line depicts the $j(V)$-characteristic of a Pt-contact sputtered in Argon. Room temperature $j(V)$-characteristics of reactively sputtered Au, Pd, and Pt Schottky barrier contacts on (b) UID, (c) Mg-, and (d) Sn-doped In_2O_3 thin films. The (dashed) lines are model curves calculated considering thermionic emission (TE) and the series resistance of the diode. The grey line in (b) is the characteristic of an Pt contact that was sputtered in Ar atmosphere.

cycle. For both the upward and the downward temperature ramping we determined the barrier height and ideality factor which are depicted in Fig. 2 in dependence on the inverse temperature. From the $\Phi_B^{eff}(T)$ vs. $1/T$ plot the homogeneous or mean barrier height and the standard deviation of the Gaussian broadened barrier potential are obtained.[17,18] During the heat cycle the homogeneous barrier height Φ_B^{hom} decreased from about 1.13 eV to 0.99 eV, whereas the standard deviation σ remained with 0.17 and 0.16 eV about constant. This is also reflected by the fact that the voltage dependence of the standard deviation is with about −0.046 and -0.049 eV essentially the same prior and after heating. The voltage dependence ρ_2 of the homogeneous barrier height changes consequently from 0.21 to 0.19. We emphasize that the diode undergoes irreversible changes at a temperature of 120 °C after these changes the diode is stable and fully functional up to at least 150 °C.

Now, we can compare the experimentally derived homogeneous barrier height to values predicted within the metal-induced gap state (MIGS) and electronegativity concept:[20]

$$\Phi_B^{hom} = \Phi_{bp}^n + S_X(X_M - X_{In_2O_3}), \quad (1)$$

where Φ_{bp}^n is the n-type branch-point energy (difference between energy of the conduction band minimum E_c and the branch-point energy E_{bp}, $\Phi_{bp}^n = E_c - E_{bp}$), S_X is the slope parameter and depends on the high-frequency dielectric constant $S_X = \Phi_B^{eff} A_X/(1 + 0.1(\varepsilon_\infty - 1)^2)$, X_M and $X_{In_2O_3}$ are the electronegativity of the contact metal and indium oxide in Miedema units. $X_{In_2O_3} = 5.73$ eV was obtained converting its Pauling scale value of 2.52 eV[21] to Miedema scale. $A_X = 0.86$ is a proportionality factor linking metal work function and the electronegativity of the metal in Miedema unit. Using the high-frequency dielectric constant $\varepsilon_\infty = 4.43$ derived from $\varepsilon_\infty \times m_{opt} = 1.24\, m_0$ and $m_{opt} = 0.28\, m_0$[22] and the experimentally determined branch-point energy of King *et al.*[5] we find for Pt/In_2O_3: $\Phi_{B,Pt}^{hom} = -0.4$ eV + 0.395 × (5.65 eV − 5.73 eV) = −0.43 eV. This actually states that a Schottky barrier should not form between Pt and In_2O_3 being in conflict with the above data. The large discrepancy between predicted and experimentally determined homogeneous barrier height is illustrated in Fig. 2(c). The dashed green area indicates values calculated using Eq. (1) for $0.1 < S_X < 0.4$ eV and $0 < E_{bp} - E_c < 0.5$ eV. The green rectangle represents the range of homogeneous barrier heights (including experimental errors) deduced for Pt/In_2O_3 from the temperature-dependent *IV* data. According to the MIGS and electronegativity concept a Schottky barrier should not form between Au, Pd, Pt, and In_2O_3, respectively. For the II-VI semiconductor ZnO a similarly large discrepancy between predicted and experimentally determined barrier heights was reported[23] and suggests revisiting the predictive power of the MIGS and electronegativity concept and/or branch-point energies. Of course, more experimental work on Schottky barrier heights on In_2O_3 is required to establish experimentally chemical trends of the barrier height for various contact metals.

For Pt/In_2O_3(UID) diode space charge spectroscopic investigations are briefly discussed. From capacitance-voltage measurements at RT a mean net doping density of 1.5×10^{17} cm^{-3} was determined, a value in excellent agreement with the Hall effect data. However, the net doping density is not constant but varies along the growth direction. This hinders an unambiguous determination of the homogeneous barrier height. Thermal admittance spectroscopy was measured in a temperature range from about 20 K to 330 K at zero bias. The temperature dependence of the diode capacitance is depicted for selected probing frequencies ω in Fig. 3. In the temperature range from 20 K to 60 K freeze-out of carriers occurs. For temperatures higher than 200 K a deep-level defect contributes to the capacitance. For the deep-level defect standard maximum evaluation of $G(\omega)/\omega$ was applied to construct the Arrhenius plot depicted in the inset of Fig. 3. The thermal activation energy and apparent capture cross-section are determined from linear regression of the Arrhenius straight line to be $E_t = 290$ meV and $\sigma_{app} = 6 \times 10^{-15}$ cm^2. For evaluation of carrier freeze-out Pautrat *et al.*[24] proposed a model that requires the temperature dependence of the carrier mobility in the temperature range in which freeze-out occurs as input.

Temperature-dependent mobility data do not exist, hence we consider ionized impurity (IIS) and grain boundary scattering (GBS) typically limiting low temperature mobility of oxide semiconducting thin films.[25,26] For IIS an unrealistically small value $E_t = 5.9$ meV is obtained and so GBS is considered. Here, the height of the potential barrier between adjacent grains enters evaluation. We have constructed an Arrhenius plot for a typical range of V_b and obtain the following $E_t(V_b)$:

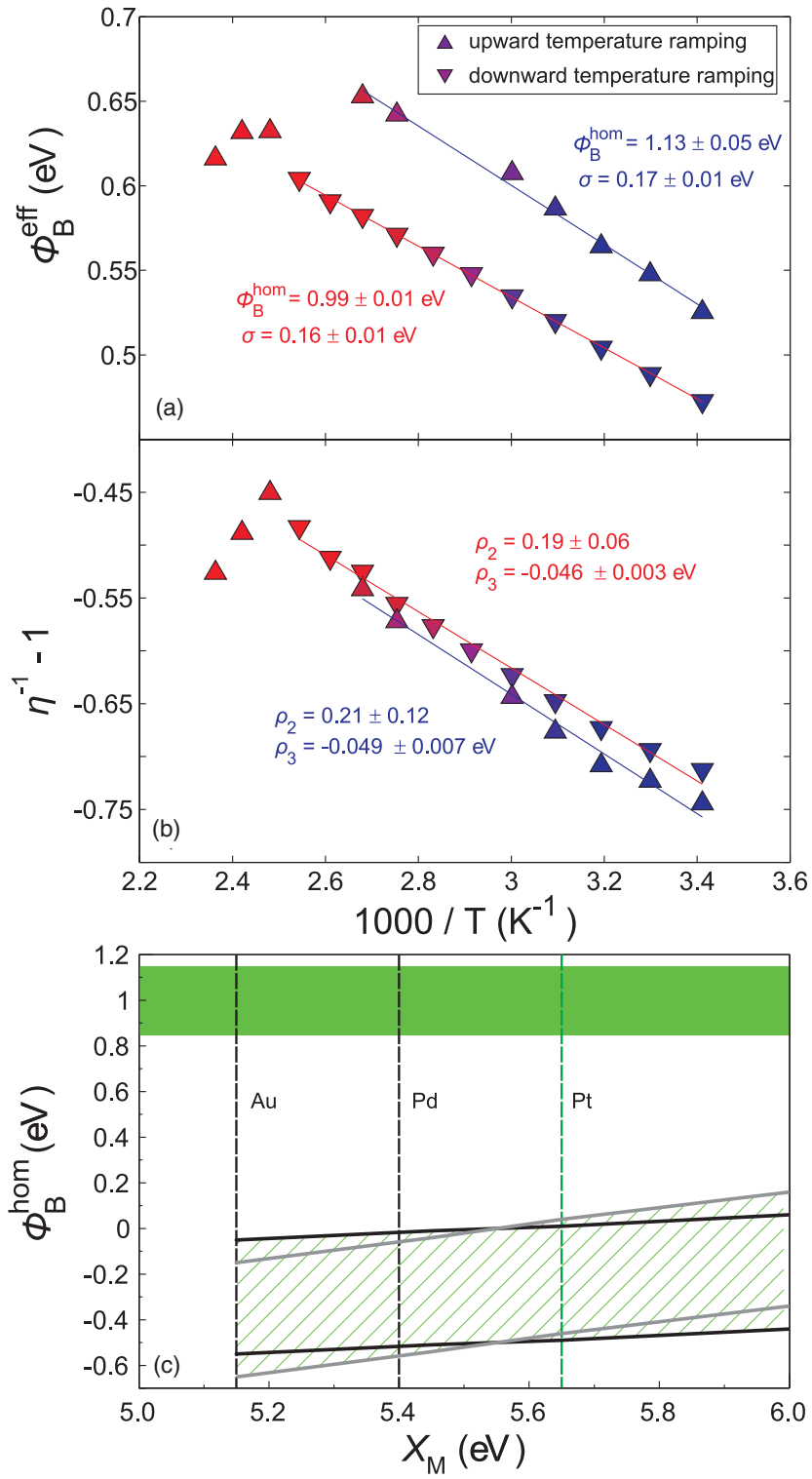

FIG. 2. (a) Effective barrier height Φ_B^{eff} and (b) ideality factor η of a Pt Schottky diode on In_2O_3:Mg in dependence on the inverse temperature. Upward (downward) directed triangles represent results obtained from upward (downward) temperature ramping. The lines are fits to the data considering the model of a Gaussian barrier height distribution.[17,18] (c) Predicted homogeneous barrier heights for 0.1 eV (black lines) $< S_X <$ 0.4 eV (grey lines) and 0 eV (upper lines) $< E_{bp} - E_c <$ 0.5 eV (lower lines) according to Eq. (1). The green box indicates the homogeneous barrier height of Pt/In_2O_3, the vertical dashed lines indicate electronegativity of Au, Pd, and Pt (from left to right). We used Miedema scale for electronegativity.

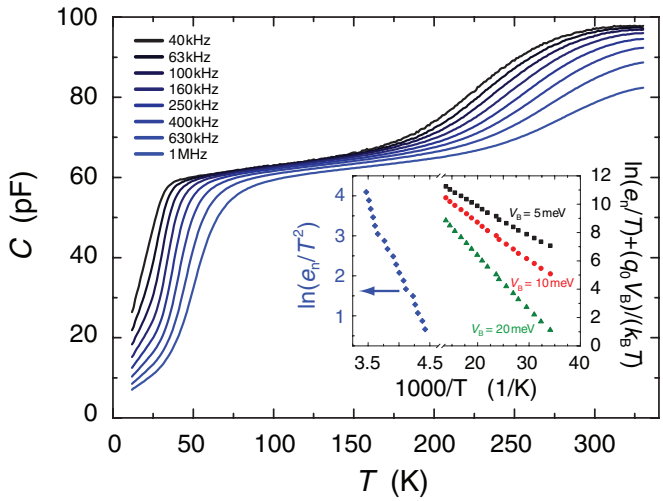

FIG. 3. Temperature dependence of capacitance of Pt/In_2O_3(UID) Schottky barrier diode for probing frequencies as labelled in the figure and zero bias. The inset depicts the Arrhenius plot of a shallow defect level freezing out below 50 K and a deeper level causing the capacitance step at about 250 K. For the shallow level we depict the Arrhenius diagram as a function of the potential barrier V_B between adjacent grains (see text for details).

$E_t(5\,\text{meV}) = 18\,\text{meV}$, $E_t(10\,\text{meV}) = 23\,\text{meV}$, and $E_t(20\,\text{meV}) = 33\,\text{meV}$. We assume the activation energy between about 25 and 30 meV.

In summary we have realized Schottky barrier contacts on UID, lightly Mg-doped and lightly Sn-Doped MBE-grown In_2O_3(001) thin film samples by a reactive sputtering process in an O_2/Ar environment. The diode current can be well described by thermionic emission across a laterally inhomogeneous barrier. Temperature-dependent measurements reveal that these barrier fluctuations can be well modeled by a Gaussian distribution. Best contacts were obtained with Pt on Mg-doped samples and showed rectification of more than three orders of magnitude, the averaged RT effective barrier height of Au, Pd, and Pt on the UID sample is 0.50, 0.49, and 0.57 eV, respectively. For Pt contacts on the Mg-doped sample changes of the contact properties were observed at 120 °C. After that, the diode was stable up to at least 150 °C and its mean barrier height was determined to be about 1 eV. The realization of first rectifying contacts to In_2O_3 enables systematic characterization of In_2O_3 by depletion region based characterization techniques and the use in unipolar field-effect devices. During the reactive sputtering process oxygen ions likely removed surface oxygen vacancies that were attributed to cause the SEAL. We note, however, that removal of the SEAL contrasts the charge neutrality picture that predicts donor type defects (the surface itself or defects caused by the O-ion damage) to move the Fermi level into the conduction band. Further insights into the effect of the oxygen ions on surface accumulation and a refined theoretical concept for predicting Schottky barrier heights on SOs like In_2O_3 or ZnO and/or additional investigations of their branch point energy are demanded.

[1] O. Bierwagen and J. S. Speck, Appl. Phys. Lett. **97**, 072103 (2010).
[2] N. Preissler, O. Bierwagen, A. T. Ramu, and J. S. Speck, Phys. Rev. B **88**, 085305 (2013).
[3] O. Bierwagen and J. S. Speck, Appl. Phys. Lett. **101**, 102107 (2012).
[4] O. Bierwagen and J. S. Speck, Phys. Stat. Sol. A **211**, 48 (2014).
[5] P. King, T. D. Veal, D. J. Payne, and A. Bourlange, Phys. Rev. Lett. **101**, 116808 (2008).
[6] B. Höffling, A. Schleife, C. Rodl, and F. Bechstedt, Phys. Rev. B **85**, 035305 (2012).
[7] A. Walsh, Appl. Phys. Lett. **98**, 261910 (2011).
[8] S. Lany, A. Zakutayev, T. O. Mason, J. F. Wager, K. R. Poeppelmeier, J. D. Perkins, J. J. Berry, D. S. Ginley, and A. Zunger, Phys. Rev. Lett. **108**, 016802 (2012).
[9] B. J. Coppa, C. C. Fulton, S. M. Kiesel, R. F. Davis, C. Pandarinath, J. E. Burnette, R. J. Nemanich, and D. J. Smith, J. Appl. Phys. **97**, 103517 (2005).
[10] H. L. Mosbacker, Y. M. Strzhemechny, B. D. White, P. E. Smith, D. C. Look, D. C. Reynolds, C. W. Litton, and L. J. Brillson, Appl. Phys. Lett. **87**, 012102 (2005).
[11] O. Bierwagen, M. E. White, M.-Y. Tsai, T. Nagata, and J. S. Speck, Appl. Phys. Exp. **2**, 106502 (2009).

[12] T. Nagata, O. Bierwagen, M. E. White, M.-Y. Tsai, and J. S. Speck, J. Appl. Phys. **107**, 033707 (2010).
[13] O. Bierwagen, J. S. Speck, T. Nagata, T. Chikyow, Y. Yamashita, H. Yoshikawa, and K. Kobayashi, Appl. Phys. Lett. **98**, 172101 (2011).
[14] A. Lajn, H. V. Wenckstern, Z. Zhang, C. Czekalla, G. Biehne, J. Lenzner, H. Hochmuth, M. Lorenz, M. Grundmann, S. Wickert, C. Vogt, and R. Denecke, J. Vac. Sci. Technol. B **27**, 1769 (2009).
[15] H. Frenzel, A. Lajn, H. von Wenckstern, and G. Biehne, Thin Solid Films **518**, 1119 (2009).
[16] A. Lajn, H. von Wenckstern, M. Grundmann, G. Wagner, P. Barquinha, E. Fortunato, and R. Martins, J. Appl. Phys. **113**, 044511 (2013).
[17] J. H. Werner and H. H. Güttler, Phys. Scr. **T39**, 258 (1991).
[18] J. H. Werner and H. H. Güttler, J. Appl. Phys. **69**, 1522 (1991).
[19] See supplementary material at http://dx.doi.org/10.1063/1.4870536 for details on current transport by thermionic emission and temperature-dependent *IV* measurements.
[20] W. Moench, J. Appl. Phys. **109**, 113724 (2011).
[21] S. Matar, G. Campet, and M. Subramanian, Prog. Sol. State Chem. **39**, 70 (2011).
[22] Y. Ohhata, F. Shinoki, and S. Yoshida, Thin Solid Films **59**, 255 (1979).
[23] M. W. Allen and S. M. Durbin, Phys. Rev. B **82**, 165310 (2010).
[24] J. L. Pautrat, B. Katircioglu, N. Magnea, D. Bensahel, J. C. Pfister, and L. Revoil, Solid-State Electron. **23**, 1159 (1980).
[25] H. von Wenckstern, M. Brandt, G. Zimmermann, J. Lenzner, H. Hochmuth, M. Lorenz, and M. Grundmann, MRS Proc. **957**, 0957–K03–02 (2006).
[26] H. von Wenckstern, M. Brandt, H. Schmidt, G. Biehne, R. Pickenhain, H. Hochmuth, M. Lorenz, and M. Grundmann, Appl. Phys. A **88**, 135 (2007).